Sliding Drops: Ensemble Statistics from Single Drop Bifurcations

Markus Wilczek,[1,2,*] Walter Tewes,[1] Sebastian Engelnkemper,[1] Svetlana V. Gurevich,[1,2,3] and Uwe Thiele[1,2,3,†]
[1]Institute for Theoretical Physics, University of Münster, Wilhelm-Klemm-Strasse 9, D-48149 Münster, Germany
[2]Center for Nonlinear Science (CeNoS), University of Münster, Corrensstrasse 2, D-48149 Münster, Germany
[3]Center for Multiscale Theory and Computation (CMTC), University of Münster, Corrensstrasse 40, D-48149 Münster, Germany
(Received 2 June 2017; published 14 November 2017)

Ensembles of interacting drops that slide down an inclined plate show a dramatically different coarsening behavior as compared to drops on a horizontal plate: As drops of different size slide at different velocities, frequent collisions result in fast coalescence. However, above a certain size individual sliding drops are unstable and break up into smaller drops. Therefore, the long-time dynamics of a large drop ensemble is governed by a balance of merging and splitting. We employ a long-wave film height evolution equation and determine the dynamics of the drop size distribution towards a stationary state from direct numerical simulations on large domains. The main features of the distribution are then related to the bifurcation diagram of individual drops obtained by numerical path continuation. The gained knowledge allows us to develop a Smoluchowski-type statistical model for the ensemble dynamics that well compares to full direct simulations.

DOI: 10.1103/PhysRevLett.119.204501

Introduction.—The coarsening of small-scale structures as, for instance, clusters, crystals, drops, or quantum dots, into larger ones is a fundamental and widely investigated physical process common in nature and technology [1,2]. Amongst the first investigations of coarsening dynamics is Ostwald's work on the growth of larger crystals or particles in solution at the expense of smaller ones [3]. Often, these processes of Ostwald ripening can be described by scaling laws for the time evolution of typical length scales. The power law scaling for cluster growth was explained by Lifshitz and Slyozov [4] and, independently, by Wagner [5]. Their derivation accounts for a key feature of such systems, namely, the coupling of the dynamics of the individual objects and of the entire ensemble.

A particular soft matter example is an ensemble of liquid drops on a solid substrate which naturally exhibits coarsening. The statistical description of condensing and coarsening drops on horizontal substrates, i.e., their evolution towards equilibrium, was addressed by Meakin and coworkers in terms of particle-based statistical models [6] and, also, by Smoluchowski-type integrodifferential equations for volume distribution functions [7]. They also consider the case of inclined substrates, where the drops are initially pinned and then depin at a critical volume in an avalanche process. The coarsening and migration of liquid drops on horizontal substrates was also addressed in detail for the one- (1D) [8–11] and two-dimensional (2D) cases [12,13] employing a lubrication or long-wave model [14,15]. The relation to Ostwald ripening is also discussed in [16].

Here, we analyze the coarsening dynamics of liquid drops that, due to gravitation, slide down a plate of fixed inclination. The lateral motion of the drops with respect to each other depends strongly on differences in drop size resulting in a fast relative transport that facilitates coarsening, i.e., the coalescence of smaller drops into larger ones. At the same time, large drops above a certain critical size are unstable with respect to breakup into smaller ones, due to the so-called pearling instability. Similarly, drops of fixed size are unstable above a critical substrate inclination [17,18]. We investigate the interplay of the accelerated coarsening and the pearling instability and elucidate the resulting statistical properties of large ensembles of sliding drops. To this end, we employ a long-wave film height evolution equation and conduct large-scale direct numerical simulations (DNS) of sliding drop ensembles to extract the dynamics of statistical measures like the drop size distribution. Next, the resulting stationary distribution of the ensemble is related to the bifurcation diagram and stability properties of individual drops obtained by numerical path continuation techniques [19]. Finally, we merge the numerically obtained single-drop information including several scaling laws and develop an augmented Smoluchowski coagulation equation as a simple statistical model that describes the dynamics of the drop size distribution.

Modelling and numerical implementation.—A nondimensional long-wave equation is used to model the time evolution of the height profile $h(x, y, t)$ that describes drops of a simple liquid on a partially wetting substrate, cf. [18]

$$\partial_t h = -\nabla \cdot \left[\frac{h^3}{3} \nabla(\Delta h + \Pi(h)) + \frac{h^3}{3} G \begin{pmatrix} \alpha \\ 0 \end{pmatrix} \right]. \quad (1)$$

The model accounts for the surface tension of the liquid via a Laplace pressure, substrate-liquid interactions such as wettability via a Derjaguin (or disjoining) pressure $\Pi(h) = -1/h^3 + 1/h^6$, and for the lateral driving where G

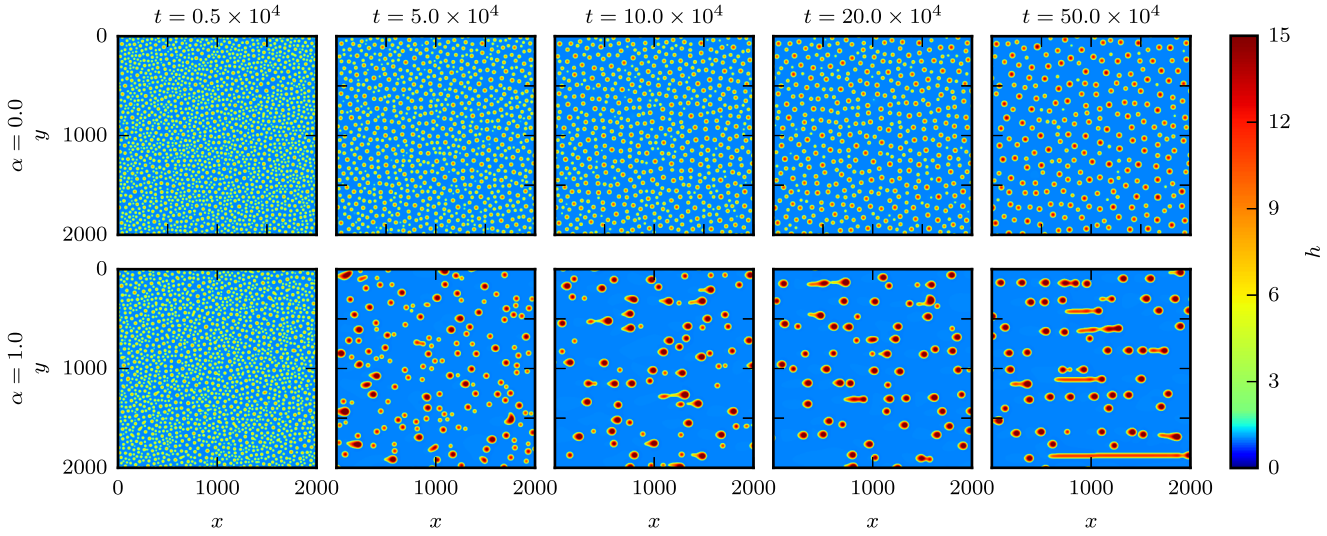

FIG. 1. Snapshots at different times t from DNS of the model (1) for (top) horizontal $\alpha = 0$ and (bottom) inclined $\alpha = 1$ substrates. The drops slide from left to right and only one quarter of the computational domain is shown. The Supplemental Material [25] contains the corresponding videos.

and α are a nondimensional gravity parameter and the inclination angle of the substrate, respectively [20]. The employed Derjaguin pressure [21] results in the presence of a thin adsorption layer in the whole domain on which the drops slide. DNS of this model are conducted on a large spatial domain $\Omega = [0, 4000] \times [0, 4000]$ with periodic boundary conditions using a finite-element method on a quadratic mesh with bilinear ansatz functions and a second-order implicit Runge-Kutta scheme for time stepping, implemented using the DUNE PDELAB framework [22–24] with a homogeneous linearly unstable liquid layer of height $h_0 = 2.0$ with small-amplitude noise as initial conditions (for more numerical details see [18]).

Properties of the drop ensembles.—Figure 1 presents simulation snapshots at different times t that contrast coarsening on a horizontal ($\alpha = 0$, top row) and an inclined ($\alpha = 1.0$, bottom row) substrate. Up to $t \approx 0.5 \times 10^4$, the coarsening proceeds very similarly in both cases; however, at a nonzero inclination, the later stages are dominated by a faster coarsening process that results in larger drop sizes. This continues until a certain time ($t_c \approx 6.5 \times 10^4$ at $\alpha = 1.0$), after which the typical drop size hardly increases further, because the pearling instability breaks up all drops above a certain volume. Only at very late stages of the simulation can a tendency to form large elongated drops be noted.

To quantify the coarsening process, we use the total number of drops $N_D(t)$ in the domain [26], as well as the drop size distribution $f(V, t)$ obtained by a Gaussian kernel density estimation (KDE) (see [27,28]). In this description, $N_{[V,V+dV]} = f(V)dV$ is the number of drops with a volume in the interval $[V, V + dV]$. Figure 2 shows the time evolution of the normalized drop size distribution $\tilde{f}(V, t) = f(V, t)/N_D(t)$ in the inclined case of Fig. 1 ($\alpha = 1.0$), while the change in the total number of drops $N_D(t)$ is presented for various inclinations in Fig. 5 (bottom panel, solid lines). We find, that the inclination-induced acceleration of coarsening results in a fast drop number decrease. In particular, this coarsening is always faster than the rigorous scaling law $N_D(t) \sim t^{-3/4}$ which presents an upper bound for any case with zero inclination [13], and further accelerates with increasing inclination. In the drop size distribution (cf. Fig. 2), the fast coarsening is visible as a

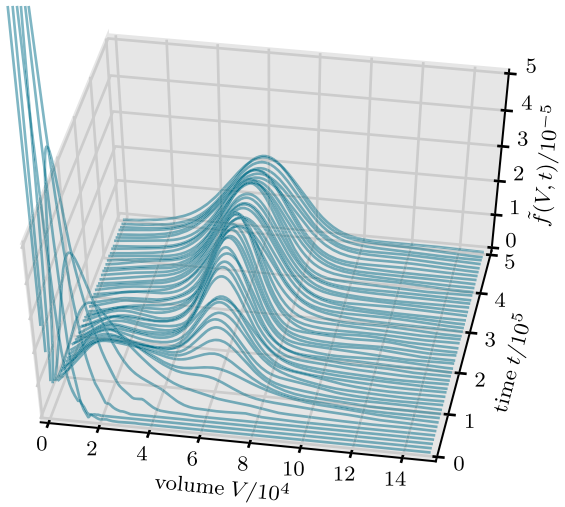

FIG. 2. Time evolution of the normalized drop size distribution $\tilde{f}(V, t)$ obtained at each time step by KDE for the DNS in the lower row of Fig. 1. In the early stage, the sharp peak at small drop volumes slowly broadens and shifts to the right. At later times, a second maximum at larger volumes appears, grows, broadens, and becomes dominant before it finally reaches an almost steady shape.

strong broadening and shifting of the initially tightly peaked distribution towards larger volumes. Around $t \approx 1 \times 10^5$, it then develops a second local maximum at $V \approx 6 \times 10^4$, which grows in time at the cost of drops with smaller volumes. Finally, after an inclination-dependent time t_c, the coarsening almost stops, as indicated by a significant kink in the $N_D(t)$ curve (Fig. 5, bottom) and a subsequent very slow decrease. In the DNS (see Fig. 1), this phase occurs for $t > t_c \approx 6.5 \times 10^4$ and is characterized by drop ensembles consisting of similar-sized drops, in accordance with the quite uniform and almost stationary drop size distribution (Fig. 2). Therefore, the drops slide with small relative velocities, leading to only a few coalescence events. These mergings often result in large drops that are unstable with respect to pearling and breakup again. In this way, statistically, an almost stationary state is reached and kept in which merging and breakup of drops balance.

Stability properties of single drops.—The time evolution of the drop size distribution results from the interplay of drop interactions (dominated by their relative velocity) and stability properties of individual drops. Information for both is presented in Fig. 3 in the form of a bifurcation diagram obtained by pseudoarclength continuation within the PDE2PATH framework [29]. It shows the dependence of sliding velocity on drop volume V for a single drop at fixed inclination (cf. Ref. [18] for other cases and implementation details). Figure 3 reveals the existence of a variety of different drop shapes, velocities, and stability properties. For small drop volumes V, only simple, almost ellipsoidal cap-shaped drops exist [sub-branch (a)]. Increasing V, this sub-branch terminates at a critical volume $V_{cr} \approx 7.2 \times 10^4$ in a saddle-node bifurcation, which also connects it to sub-branch (b), whose drops exhibit an elongated tail and are linearly unstable. Sub-branch (b) connects to the stable sub-branches (c) and (d) via another saddle-node bifurcation and a subsequent Hopf bifurcation (cf. [18]). Although at small volumes, only the drops of sub-branch (a) exist, from $V \approx 5.3 \times 10^6$ onwards, we find a multistability of sub-branch (a) and the elongated drops of sub-branch (c). In the DNS, one mainly observes drops from sub-branch (a) because most drops with $V > V_{cr}$ that are formed by merging are unstable and decay by pearling. However, very seldom is a merged drop elongated and linearly stable, i.e., on sub-branches (c) and (d).

Next, we connect the information gained from the bifurcation study of the individual drop to the ensemble dynamics. As at relatively low inclinations stable elongated drops are rarely formed, we focus on sub-branch (a): The bifurcation point at V_{cr} provides the stability limit for simple drops and, therefore, sets an upper limiting volume for the ensemble DNS. Figure 4 shows bifurcation curves together with the late-stage quasistationary drop size distributions obtained from DNS. Comparison shows, that the location of the main peak of the distribution is directly connected to the position of the saddle-node bifurcation at V_{cr}: The number of drops with $V > V_{cr}$ decreases significantly. Indeed, V_{cr} almost coincides with the rhs inflection point of the size distribution. These observations equally hold for different inclinations α (see Fig. 4).

Further, we extract power laws that relate (i) drop velocity to drop volume and inclination angle from single-drop bifurcation diagrams as the one in Fig. 3 (for details see [18])

$$U(V) = a_0 \alpha V^{\beta_0}, \tag{2}$$

and (ii) critical volume V_{cr} to inclination angle

$$V_{cr} = a_1 \alpha^{\beta_1}, \tag{3}$$

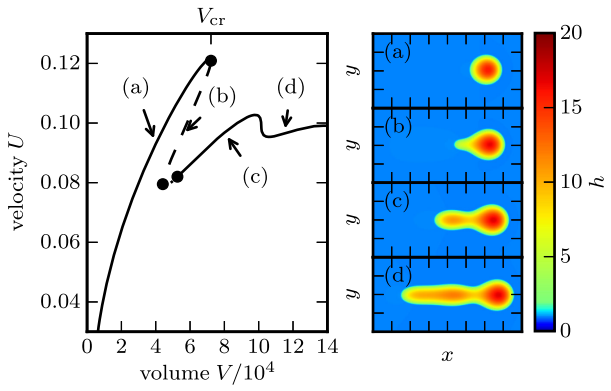

FIG. 3. (left) Bifurcation diagram of sliding drops [modeled by Eq. (1)] on a substrate with inclination $\alpha = 1.0$. Shown is the sliding velocity U in dependence on the drop volume V. There exist several sub-branches of stationary drops with different shape and behavior, see labels (a) to (d) and the corresponding solutions on the right.

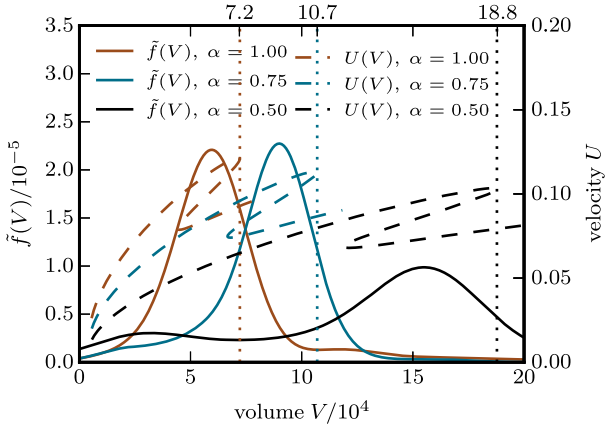

FIG. 4. Comparison of late-stage quasistationary normalized drop size distributions $\tilde{f}(V)$ at $t = 5 \times 10^5$ and bifurcation diagrams $U(V)$ for single drops at different fixed inclinations α. The vertical dotted lines indicate the position V_{cr} of the respective saddle-node bifurcation.

with $a_0 = 2.2 \times 10^{-4}$, $\beta_0 = 0.569$, $a_1 = 7.18 \times 10^4$, and $\beta_1 = -1.40$.

Statistical model.—In the final step, the obtained "single-drop" information is employed to develop a minimal statistical model for the ensemble dynamics as characterized by the unnormalized drop size distribution $f(V,t)$. To capture the coarsening dynamics that is dominated by the interplay of collision-caused merging and instability-caused splitting of drops, we extend Smoluchowski's continuous rate equation for coagulation [7], following the approach of Meakin *et al.* for breath figures (see [6] and references therein). Thereby, loss and gain of drops of each volume are accounted for through continuous transition rate kernels for coalescence and fragmentation. The model conserves the total volume and reads

$$\begin{aligned}\partial_t f(V,t) = &\underbrace{-\int_0^\infty K(V,\tilde{V}) f(V) f(\tilde{V}) d\tilde{V}}_{\text{loss due to coalescence}} \\ &\underbrace{+\int_0^V \frac{1}{2} K(\tilde{V}, V-\tilde{V}) f(\tilde{V}) f(V-\tilde{V}) d\tilde{V}}_{\text{gain due to coalescence}} \\ &\underbrace{-\int_0^\infty \frac{1}{2} J(V,\tilde{V}) f(V) d\tilde{V}}_{\text{loss due to fragmentation}} + \underbrace{\int_0^\infty J(\tilde{V},V) f(\tilde{V}) d\tilde{V}}_{\text{gain due to fragmentation}},\end{aligned} \tag{4}$$

$$\text{where } K(V_a,V_b) = \frac{2k_1}{L}|U(V_a) - U(V_b)|, \tag{5}$$

$$J(V_a,V_b) = j\sigma(V_a,V_{\text{cr}})\Theta(V_a - V_b). \tag{6}$$

The properties of the kernels K and J in this nonlocal evolution equation are crucial features of the coarse-grained model. We deduce them from the single-drop results (2) and (3) above and employ a minimum of free parameters and assumptions. In particular, the kernel $K(V_a,V_b)$ [cf. Eq. (5)] accounts for the coalescence of two drops with volumes V_a and V_b. It sets the frequency of collisions as the ratio of the relative drop velocity and the mean distance $L/2$ between two drops on the domain. The drop velocities $U(V)$ are given by the obtained scaling law (2) with the only *a priori* unknown parameter being k_1. It is a measure for the reduction of the number of collisions because all drops slide in the same direction and, therefore, only interact with a subset of the other drops. The other kernel $J(V_a,V_b)$ [cf. Eq. (6)] with the sigmoid function $\sigma(V_a,V_{\text{cr}})$ [30] accounts for drop splitting and corresponds to the simplest implementation of the instability threshold obtained above. In particular, drops with $V_a > V_{\text{cr}}$ fragment into two drops of volume V_b and $V_a - V_b$, respectively, with equal probability for all $V_b < V_{\text{cr}}$ (expressed by the Heaviside function Θ) [31]. The only free parameter j represents the time scale

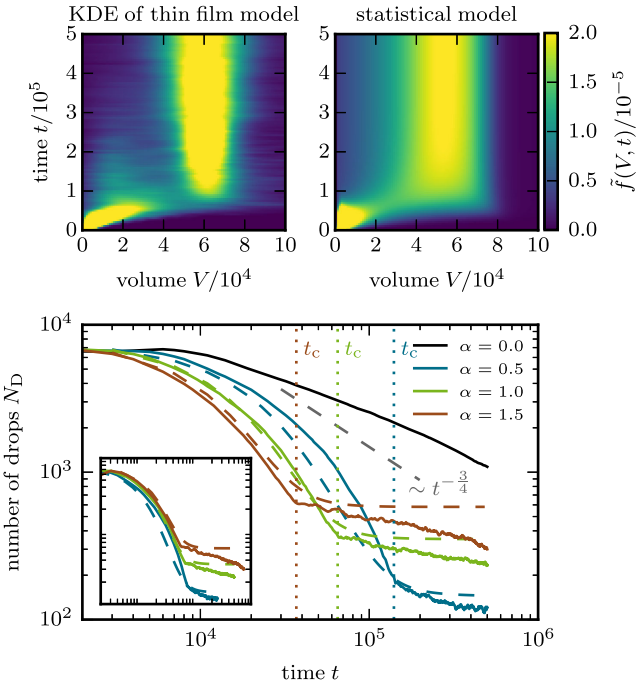

FIG. 5. (top) Space-time plots show the time evolution of the drop size distribution $\tilde{f}(V,t)$ at $\alpha = 1.0$ obtained by KDE from (left) a DNS of Eq. (1) (cf. Fig. 2) and (right) a simulation of the statistical model (4). (bottom) Comparison of the time evolution of the drop number $N_D(t)$ for different inclinations α as obtained by DNS (solid lines) and statistical model (dashed lines). The coarsening with inclination is always faster than the rigorous upper bound $N_D(t) \sim t^{-3/4}$ valid for horizontal substrates [13]. The inset shows the same data with the t axis scaled by α, which results in a master curve in the collision-dominated regime. The remaining parameters are $j = 6.25 \times 10^{-6}$, $k_1 = \frac{1}{30}$.

ratio between fragmentation and coalescence processes. Note that the statistical model (4) neglects the classical Ostwald ripening, i.e., coarsening by diffusive mass transfer between drops as, even at extremely small inclination, the considered coarsening by drop translation is much faster.

The developed statistical model (4) is solved numerically [32] employing initial conditions corresponding to early stages of the DNS of Eq. (1) (e.g., in Fig. 1). As a result, the top row of Fig. 5 compares the two dynamics of the drop size distribution as measured in the DNS of the thin film equation (1) and in the simulation of the statistical model (4). It shows a very good agreement of all main features, as, e.g., the appearance of a second peak and the convergence to a quasistationary distribution.

Furthermore, the bottom panel of Fig. 5 compares the evolution of the drop number N_D for different inclination angles α fixing, in all cases, parameters k_1 and j such that a best fit results for simulations with $\alpha = 1.0$. Nevertheless, the predictions of the statistical model for all inclinations agree very well with the DNS results. This gives clear evidence that the dynamics of the ensemble properties resulting from many individual complex coalescence and

fragmentation processes can be rather well captured by our simple statistical model.

Conclusions.—We have investigated the coarsening behavior of ensembles of interacting sliding drops employing a thin-film equation. We have shown, in direct numerical simulations, that the statistical ensemble properties converge to an almost stationary state corresponding to a balance of coalescence and fragmentation events. The emerging distribution can be related to stability properties of individual drops as captured in single-drop bifurcation diagrams. Further, based on the gained single-drop information, we have developed a minimal statistical model that faithfully captures the main ensemble dynamics and very well compares to the full direct numerical simulations. We believe that the proposed methodology of employing "microscopic" information in the form of bifurcation properties of individual entities (here, drops), to derive coarse-grained "macroscopic" statistical models for the ensemble dynamics, represents a multiscale approach that will prove useful in other nonlinear nonequilibrium systems.

We acknowledge partial support by Deutsche Forschungsgemeinschaft within PAK 943 (Project No. 332704749), and German-Israeli Foundation for Scientific Research and Development under Grant No. I-1361-401.10/2016.

*markuswilczek@uni-muenster.de
†u.thiele@uni-muenster.de

[1] A. Bray, Theory of phase-ordering kinetics, Adv. Phys. **43**, 357 (1994).
[2] A. Nepomnyashchy, Coarsening versus pattern formation, C.R. Phys. **16**, 267 (2015).
[3] W. Ostwald, *Lehrbuch der Allgemeinen Chemie* (Leipzig, Germany, 1896), Vol. 2.
[4] I. M. Lifshitz and V. V. Slyozov, The kinetics of precipitation from supersaturated solid solutions, J. Phys. Chem. Solids **19**, 35 (1961).
[5] C. Wagner, Theorie der Alterung von Niederschlägen durch Umlösen (Ostwald-Reifung), Ber. Bunsenges. Physik. Chem. **65**, 581 (1961).
[6] P. Meakin, Droplet deposition growth and coalescence, Rep. Prog. Phys. **55**, 157 (1992).
[7] M. V. Smoluchowski, Drei Vorträge über Diffusion, Brownsche Bewegung und Koagulation von Kolloidteilchen, Z. Phys. **17**, 557 (1916).
[8] M. Gratton and T. Witelski, Transient and self-similar dynamics in thin film coarsening, Physica (Amsterdam) **238D**, 2380 (2009).
[9] G. Kitavtsev and B. Wagner, Coarsening dynamics of slipping droplets, J. Eng. Math. **66**, 271 (2010).
[10] G. Kitavtsev, Coarsening rates for the dynamics of slipping droplets, Eur. J. Appl. Math. **25**, 83 (2014).
[11] K. B. Glasner and T. P. Witelski, Coarsening dynamics of dewetting films, Phys. Rev. E **67**, 016302 (2003).
[12] L. M. Pismen and Y. Pomeau, Mobility and interactions of weakly nonwetting droplets, Phys. Fluids **16**, 2604 (2004).
[13] F. Otto, T. Rump, and D. Slepcev, Coarsening rates for a droplet model: Rigorous upper bounds, SIAM J. Math. Anal. **38**, 503 (2006).
[14] A. Oron, S. H. Davis, and S. G. Bankoff, Long-scale evolution of thin liquid films, Rev. Mod. Phys. **69**, 931 (1997).
[15] U. Thiele, Structure formation in thin liquid films, in *Thin Films of Soft Matter*, edited by S. Kalliadasis and U. Thiele (Springer, Wien, 2007), pp. 25–93.
[16] K. Glasner, F. Otto, T. Rump, and D. Slepcev, Ostwald ripening of droplets: The role of migration, Eur. J. Appl. Math. **20**, 1 (2009).
[17] T. Podgorski, J.-M. Flesselles, and L. Limat, Corners, cusps, and pearls in running drops, Phys. Rev. Lett. **87**, 036102 (2001).
[18] S. Engelnkemper, M. Wilczek, S. V. Gurevich, and U. Thiele, Morphological transitions of sliding drops: Dynamics and bifurcations, Phys. Rev. Fluids **1**, 073901 (2016).
[19] H. A. Dijkstra, F. W. Wubs, A. K. Cliffe, E. Doedel, I. F. Dragomirescu, B. Eckhardt, A. Y. Gelfgat, A. Hazel, V. Lucarini, A. G. Salinger, E. T. Phipps, J. Sanchez-Umbria, H. Schuttelaars, L. S. Tuckerman, and U. Thiele, Numerical bifurcation methods and their application to fluid dynamics: Analysis beyond simulation, Commun. Comput. Phys. **15**, 1 (2014).
[20] Starting from a dimensional form $\tilde{\Pi}(\tilde{h}) = -A/\tilde{h}^3 + B/\tilde{h}^6$ for the disjoining pressure, we employ scales $h_{\mathrm{eq}} = (B/A)^{1/3}$ for height, $l_0 = \sqrt{3}h_{\mathrm{eq}}/\sqrt{5}\theta_{\mathrm{eq}}$ for lateral lengths, and $t_0 = 9\eta h_{\mathrm{eq}}/25\gamma\theta_{\mathrm{eq}}^4$ for time. Then $\theta_{\mathrm{eq}} = \sqrt{3A/5\gamma h_{\mathrm{eq}}^2}$ is the equilibrium contact angle and $G = 3\rho g h_{\mathrm{eq}}^2/5\gamma\theta_{\mathrm{eq}}^2$ is the gravitation number. Here, we use $G = 10^{-3}$.
[21] L. M. Pismen, Nonlocal diffuse interface theory of thin films and the moving contact line, Phys. Rev. E **64**, 021603 (2001).
[22] P. Bastian, F. Heimann, and S. Marnach, Generic implementation of finite element methods in the distributed and unified numerics environment (DUNE), Kybernetika **46**, 294 (2010).
[23] P. Bastian, M. Blatt, A. Dedner, C. Engwer, R. Klöfkorn, M. Ohlberger, and O. Sander, A generic grid interface for parallel and adaptive scientific computing. Part I: abstract framework, Computing **82**, 103 (2008).
[24] P. Bastian, M. Blatt, A. Dedner, C. Engwer, R. Klöfkorn, R. Kornhuber, M. Ohlberger, and O. Sander, A generic grid interface for parallel and adaptive scientific computing. Part II: implementation and tests in DUNE, Computing **82**, 121 (2008).
[25] See Supplemental Material at http://link.aps.org/supplemental/10.1103/PhysRevLett.119.204501 for videos of the direct numerical simulations of drop ensembles on horizontal and inclined substrates.
[26] As the height profile $h(x, y, t)$ is a single, continuous field, we define an individual drop as a connected area Ω_{drop} where the height exceeds a threshold slightly above the height of the adsorption layer (here, $h_{\mathrm{thresh}} = 1.05$).
[27] To obtain $f(V, t)$, at each step of the DNS, the volume V of each drop is calculated by integrating the height profile

$h(x, y, t)$ over the corresponding footprint Ω_{drop}. From the resulting list at time t, we calculate $f(V, t)$ using a KDE [28].

[28] D. W. Scott, *Multivariate Density Estimation: Theory, Practice, and Visualization*, 2nd ed. (John Wiley & Sons, Hoboken, New Jersey, 2015).

[29] H. Uecker, D. Wetzel, and J. D. M. Rademacher, pde2path -a matlab package for continuation and bifurcation in 2d elliptic systems, Numer. Math. **7**, 58 (2014).

[30] We use $\sigma(V_a, V_{\text{cr}}) = \frac{1}{2}\{1 + \tanh[V_a - (V_{\text{cr}} + 2b_V)/b_V]\}$ with the smoothness parameter $b_{\text{V}} = V_{\text{cr}}/10$ of the transition to the unstable regime.

[31] This simple choice is rational as information about individual instability time scales and fragmentation ratios for specific drop sizes are difficult to obtain and too complex for a simple model [18].

[32] Discretized on the volume domain and with a fourth-order Runge-Kutta time-stepping scheme.